16th World Conference on Earthquake, 16WCEE 2017
Santiago Chile, January 9th to 13th 2017
Paper N°4721 (Abstract ID)
Registration Code: S-D1464411873

STRUCTURAL PERFORMANCE OF WELD JOINTS WITH LACK-OF-FUSION DEFECT AT 35° GROOVE FACE

T. Almunyif[1], S. Minami[2], K. Hattori[3]

[1] Graduate Student, Tokyo Denki University, Japan, 15rmg01@ms.dendai.ac.jp
[2] Professor, Tokyo Denki University, Japan, minamis@g.dendai.ac.jp
[3] Tsukuba Building Test Laboratory of Center for Better Living, Japan, hattori@tbtl.org

Abstract

The characteristics of a welding joint greatly influence seismic performance in steel structure buildings. Welding defects are well known to reduce the strength capacity and elongation of welding joint in steel structures. One of the welding defects is the lack-of-fusion occurring at a groove face in a welding joint. The lack-of-fusion defect might become the fracture origin when it is located near the welding joint surface. The influence of the lack-of-fusion at the groove face is experimentally investigated in this study.

A series of cyclic bending loading tests was conducted on specimens with different defect sizes and shapes. How the defects influenced the fracture behavior was examined. The study object is the model with a defect along the groove face with a groove angle of 35°. The defect was artificially made in the specimen flange plate by electric spark machining. The defect position was the flange plate surface. The test parameters were the defect position (flange plate edge or center), size (length and depth), and face angle (35° or 0°). The specimens were made from 490 MPa class steel plate with a thickness of 25 mm.

A hydraulic-type testing machine with 1000 kN capacity was used for this loading. The specimen was tied to jig-beams with high-tension bolts as a simple beam type. The bending moment was then loaded to the specimen through a loading beam following the two-point loading procedure. Applying the bending moment to the specimen was considered to increase stress on the defect located near the surface. The loading was controlled by displacement at the specimen center. The loadings were applied following the incremental amplitude procedures until fracture. The test temperature was set to 0°C.

The summaries of the test result are as follows: a ductility crack occurred from the artificial defect, and the crack progressed with the cyclic loading, finally caused to the fracture; the relationships of the defect size between the maximum strength and the energy absorption capacity were obtained; and the allowable size of the edge defect was half the size of the center defect. The difference in the angles for the defects in the surface side is hardly observed.

Keywords: *fracture, incomplete fusion, weld defect, energy absorption capacity, cyclic loading test*

1. Introduction

Welding defects are considered to affect joint strength and deformation. One of the welding defects is the lack-of-fusion that occurs in the groove surface. The lack-of-fusion defect might trigger the initiation point of fracture when it is located near the welding joint surface [1]. The influence of the lack-of-fusion at the groove face was experimentally investigated in this study. We performed cyclic bending loading tests on specimens with different defect sizes, angles, and positions to clarify how the defects affect the fracture behavior of a welded joint.

2. Test specimens

Fig. 1 shows the specimen configurations. Each specimen is directed to a model, which has a welding defect having a 35°or 0° angle along the groove face located in the surface and the bottom side. The defect positions are the flange plate center and side edge, which are called the center defect and the edge defect, respectively. The bottom side is obtained by assuming a defect in the initial layer of a butt-welded joint. Fig. 2 shows this defect position. Table 1 presents the defect dimensions, sizes, and rates. The artificial defect was made in the specimen flange plate with 140 mm width, 300 mm length, and 25 mm thickness of the SN490B steel plate by electric spark machining. Accordingly, a clarification was made in this study from the geometric point of view, which includes aspects of defect position and shape. Series 1[2] and 2[3] used SN490B steel materials of different lots (Table 2).

Table 1 – Test specimen and result

	No.	Defect position	Defect plane	Defect angle	Defect size(mm)			Area	Defect rate	Pmax	δmax	ηs	η	Fracture cycle
					Height	Length	Width	mm^2	%	kN	mm			
Series 1	1	Center defect	Surface side	35°	1.2	100	0.4	120	4.8%	387	45.4	12.8	47.8	8
	2				2.5	28	0.4	70	2.8%	393	45.6	12.6	48.1	9
	3				5	14	0.4	70	2.8%	397	45.8	12.9	45.1	9
	4				5	28	0.4	140	5.6%	359	45.6	5.8	33.1	8
	5				10	23	0.6	230	9.2%	336	34.0	7.1	27.8	7
	6				20	38	1.0	760	30.4%	259	22.5	2.3	10.3	5
	7				25	10	1.0	250	10.0%	351	36.8	6.3	29.0	7
	8	Edge defect	Surface side	35°	2.5	14	0.4	35	1.4%	397	45.6	16.6	61.2	9
	9				5	7	0.4	35	1.4%	402	49.8	15.7	64.1	9
	10				5	14	0.4	70	2.8%	382	45.5	13.6	38.9	8
	11				10	11.5	0.6	115	4.6%	361	34.5	7.4	21.7	6
	12				20	19	1.0	380	15.2%	278	23.0	2.3	12.2	6
	13				25	5	1.0	125	5.0%	364	29.2	6.2	19.6	7
Series 2	14	Edge defect	Surface side	35°	10	10	0.6	100	4.0%	371	45.2	9.4	31.9	7
	15		Surface side	0°	10	10	0.6	100	4.0%	372	39.9	9.4	40.8	8
	16		Bottom side	0°	10	10	0.6	100	4.0%	383	47.0	12.4	52.3	9
	17	Center defect	Surface side	35°	10	20	0.6	200	8.0%	359	36.5	8.2	35.7	7
	18		Surface side	0°	10	20	0.6	200	8.0%	361	35.6	8.7	35.0	8
	19		Bottom side	0°	10	20	0.6	200	8.0%	365	36.1	9.2	41.5	8

- Pmax: maximum load.
- δmax: maximum displacement (at 90% of the maximum load).
- ηs: cumulative plastic deformation calculated from the skeleton curve (positive-loaded side; up to the maximum load).
- η: cumulative plastic deformation (positive-loaded side; up to 90% of the maximum load).
- Elastic displacement at the full plastic moment (computed value) δp = 7.1 mm (Series 1), 7.3 mm (Series 2).
- Load at the full plastic moment (computed value) Pp = 245 kN (Series 1), 252 kN (Series 2).
- All plastic moments are computed using the yield point of the material test results at 0°C.

Table 2 – Mechanical properties of steel materials

Series	Steel material	t	σy	σu	EL.	Y.R.	vEo
		mm	N/mm²	N/mm²	%	%	J
Series 1	SN490B	25	377	519	31	72.0	235
Series 2			401	542	28	74	240

- t: plate thickness; σ_y: yield point; σ_u: tensile strength; EL: elongation; Y.R.: yield ratio; and $_vE_0$: Charpy absorbed energy at 0°C.

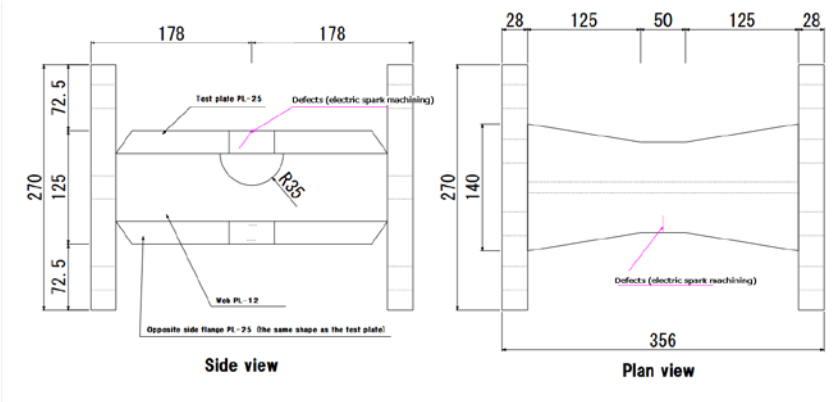

Fig. 1 – Test specimen

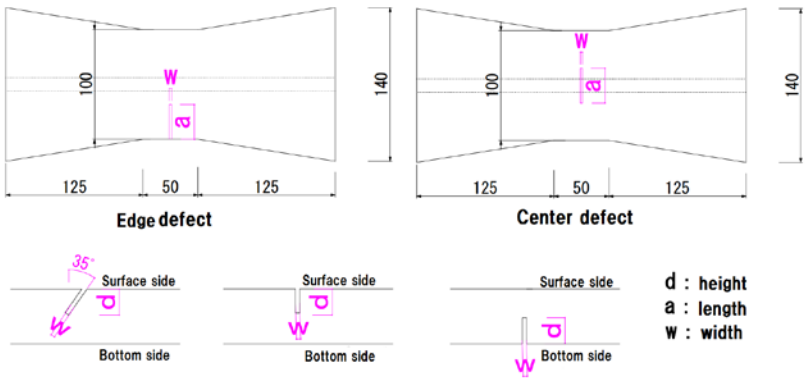

Fig. 2 – Defect angle and position

3. Experimental method

A hydraulic-type testing machine with 1000 kN capacity was used for this loading. As shown in Fig. 3, the specimen was tied to jig-beams with high-tension bolts as a simple beam type. The bending moment was applied to the specimen through a loading point beam following the two-point loading procedure. The loading was controlled by the global center displacement (δ). The displacement was computed using the following equation:

$$\delta = D3 - (D1 + D5) / 2 \quad (1)$$

Where, D1 ~ D5 are measured values of displacement transducers shown in Fig. 3.

The loading was alternately repeated as positive and negative and applied following the incremental amplitude procedures. The displacement amplitudes were ±11.3 mm, ±22.6 mm, ±33.9 mm and ±45.2 mm for Series 1; and ±12 mm, ±24 mm, ±36 mm and ±48 mm for Series 2; where the amplitudes were the even number times of the yield displacement of the specimen. The yield displacement is approximately 0.8 times of the elastic

displacement at the full plastic moment. The same amplitude was repeated twice, and pushed over when all was done.

Since steel properties vary with temperature, if intended for fracture, it is desirable to experiment at a specific temperature. The value of toughness is provided at 0 °C for building structural steels in Japanese standard. Recently this temperature has set commonly in the case of fracture tests, therefore the test temperature was set at 0 °C in this experiment. The specimen was cooled by contact with ethanol cooled by dry ice particles as refrigerant.

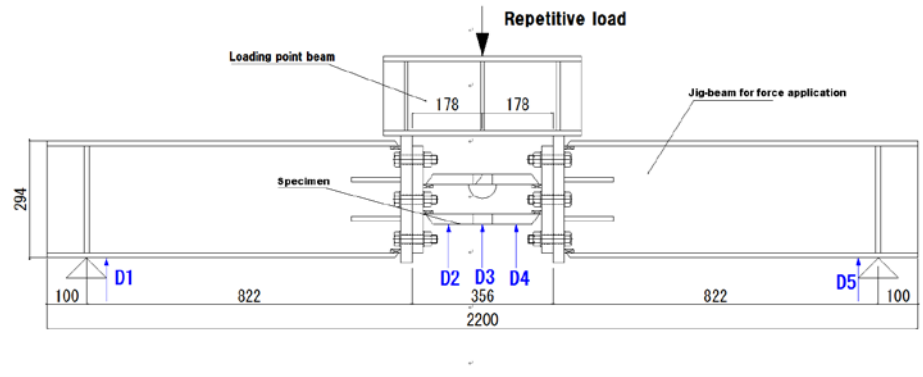

Fig. 3 – Loading setup and measurement locations

4. Experimental results

The experimental results are shown in Table 1. Figs. 4 and 5 present the load–displacement relations and skeleton curves, respectively. Specimen No. 1–No. 7 had a center defect, whereas No. 8–No. 13 had an edge defect for Series 1. Photos of some fractured specimens are shown in Photo 1.

Specimen of No. 2, No. 9, No. 10 and No. 11 showed a rapidly decreased load and a brittle fracture. The other specimens had a slowly reduced load and a ductile fracture. The largest defect rate was found in specimen No. 6, which was fractured in five cycles with early crack progress. Specimen of No. 3, No. 8 and No. 9 with a small defect rate in the center and edge defects did not fracture in ±45.2 mm. Therefore, these specimens were fractured with the push-over. Specimen No. 2 did not fracture in 45.2 mm after the second time. The specimen was rapidly fractured by increasing the load on the positive side of the push-over. Specimen No. 16 with an edge defect in Series 2 also did not fracture in ±48 mm. The specimen showed a ductile fracture by increasing the load on the positive side of the push-over.

No.14 (Surface, Edge, 35°) No. 15 (Surface, Edge, 0°) No. 18 (Surface, Center, 0°)

Photo. 1 – Fracture condition

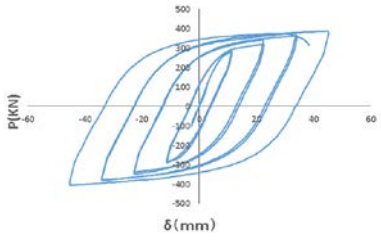

No. 1

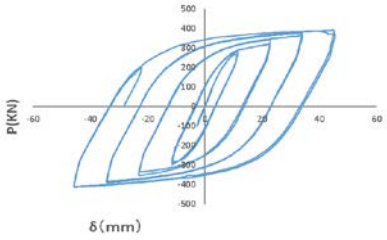

No. 2

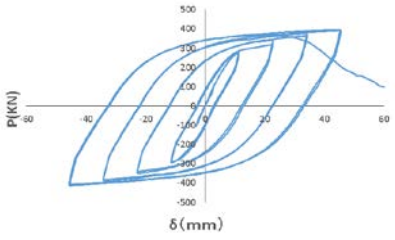

No. 3

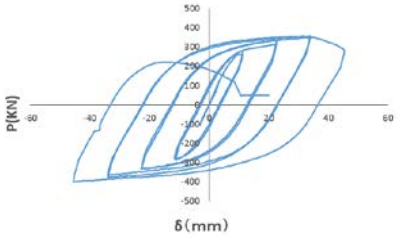

No. 4

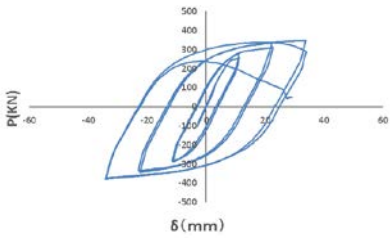

No. 5

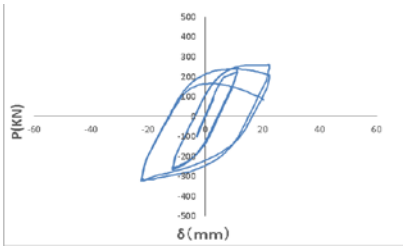

No. 6

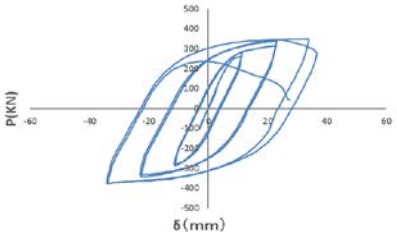

No. 7

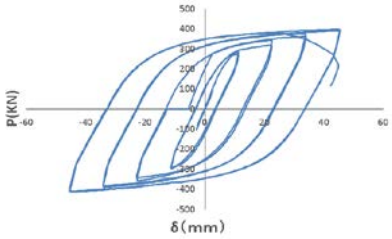

No. 8

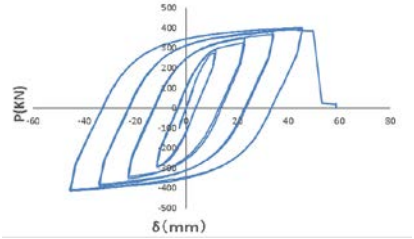

No. 9

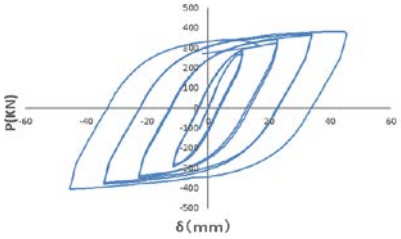

No. 10

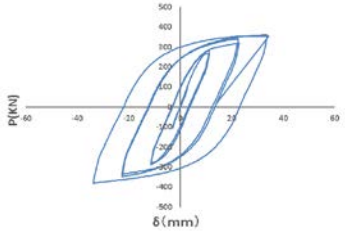

No. 11

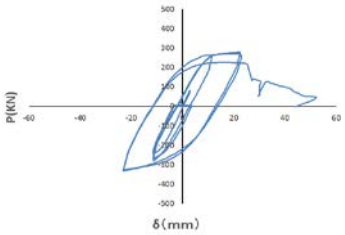

No. 12

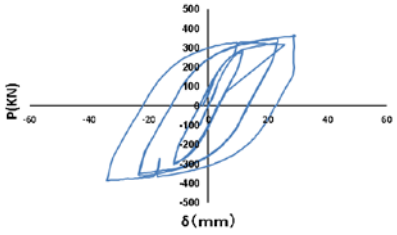

No. 13

Fig. 4 (a) – Load–displacement relationship (Series 1)

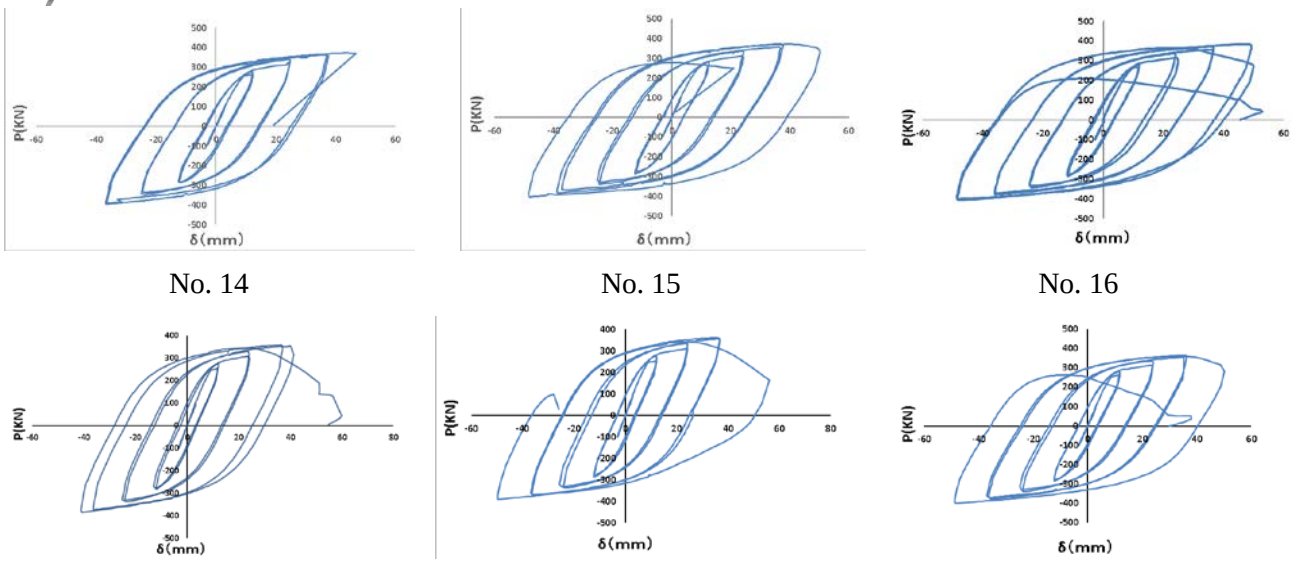

No. 14 No. 15 No. 16

No. 17 No. 18 No. 19

Fig. 4 (b) – Load–displacement relationship (Series 2)

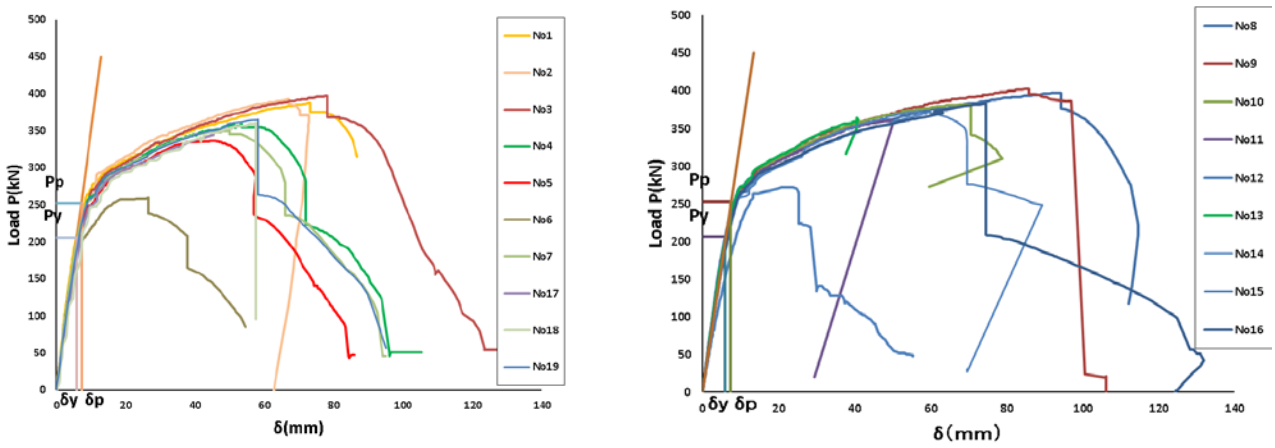

(1) Center defect (2) Edge defect

Fig. 5 – Skeleton curves

5. Discussion

The cumulative plastic deformation η can be determined by the sum of all positive load–displacement relation curve lines (= W_{total}) obtained from the experiment result by dividing with *Pp* and δp. η is the sum of up to 90% of the maximum load.

$$\eta = W_{total} / Pp\ \delta p \quad (2)$$

The cumulative plastic deformation was also determined by the skeleton curve line (ηs). Fig. 6 shows the relation between the cumulative plastic deformation and the defect rate, and Fig. 7 shows also the relation in the case of skeleton curves. The performance decreases when the defect rate is large. The higher the defect rate, the easier the specimen might fracture. The edge defect is easily fractured even with the same defect rate, which is more than that in the center defect.

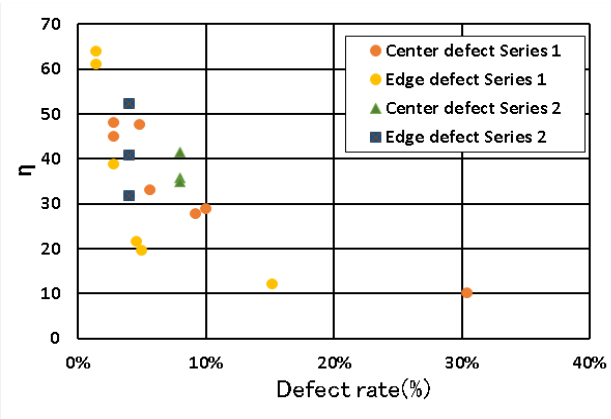

Fig. 6 – Comparison of η

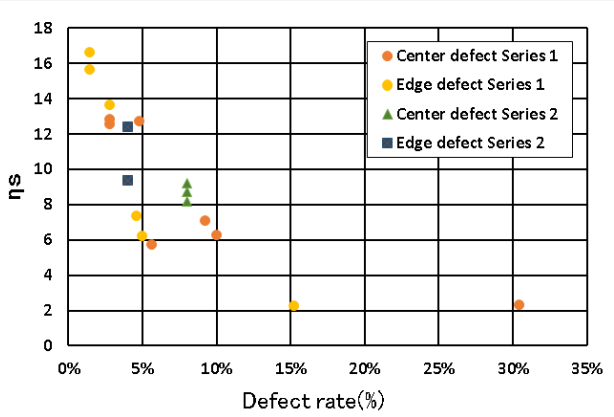

Fig. 7 – Comparison of ηs

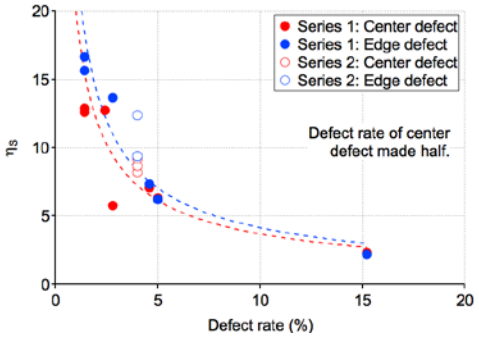

Fig. 8 – Defect rate – ηs

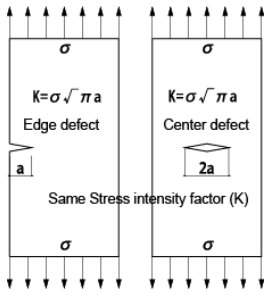

Fig. 9 – Diagram of fracture mechanics

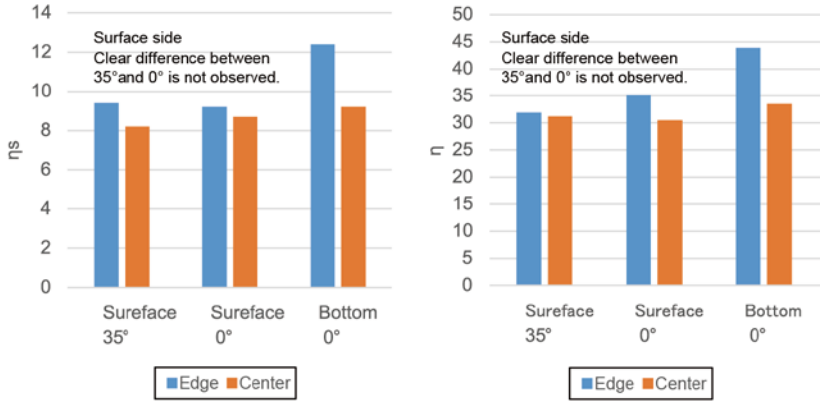

Fig. 10 – Comparison with defect angles (Series 2)

Fig. 8 is plotted with the defect rate as half values of the center defects. It appears that the results of the edge defect correspond with half the size of the center defect. From a point of view of fracture mechanics, the stress intensity factor of a edge defect of length *a* and that of a center defect of double length 2*a* are known to be equivalent [4]. The diagram of the stress intensity factor is shown in Fig. 9. It is considered that the allowable size of the edge defect is half the size of the center defect. Fig. 10 presents the comparison between different angles and between different positions of defects. Notably, η of the bottom side defect corresponding to the

initial layer defect is larger than the surface side defect even with the same defect size. The clear difference in the angles for the defects in the surface side is not observed.

6. Summary

The influence of the lack-of-fusion at the groove face was experimentally investigated. The test result summaries are as follows:

1) A ductility crack occurred from the artificial defect, and the crack progressed with the cyclic loading, finally caused to the fracture.

2) The relationships of the defect size between the maximum strength and the energy absorption capacity were obtained. The performance decreases when the defect rate is larger.

3) The same in the defect rate is considered to be easy to fracture compared with the edge defect than the center defect. The allowable size of the edge defect was half the size of the center defect.

4) The difference in the angles for the defects in the surface side is hardly observed.

7. References

[1] Kazunori Hattori, Motohiro Kasahara, Tadao Nakagomi (2014): Study on ultrasonic testing method of lack of side wall fusion at the 35 degrees groove face, *Summaries of Technical Papers of Annual Meeting*, Architectural Institute of Japan, A-1, 991–992

[2] Almunyif Thamer, Kazunori Hattori, Susumu Minami, Motohiro Kasahara (2015): Cyclic loading test of joints with lack-of-fusion defect at 35 degrees groove face (Part 1 and Part 2), *Summaries of Technical Papers of Annual Meeting*, Architectural Institute of Japan, A-1, 1043–1046

[3] Almunyif Thamer, Kazunori Hattori, Susumu Minami (2016): Cyclic loading test of joints with lack-of-fusion defect at 35 degrees groove face (Part 3), *Summaries of Technical Papers of Annual Meeting*, Architectural Institute of Japan, A-1, 12011202

[4] Yukitaka Murakami (1987): Stress intensity factors handbook, Vol. 1, Pergamon Press.